Romanian Reports in Physics, Vol. 60, No. 1, P. 27–44, 2008

Dedicated to Prof. Dorin Poenaru's
70th anniversary

DYNAMICAL STUDY OF PROTON EMISSION FROM DEFORMED NUCLEI

M. RIZEA[1], N. CARJAN[2]

[1] *"Horia Hulubei" National Institute of Physics and Nuclear Engineering*
P.O. Box MG-6, RO-077125 Bucharest-Magurele, Romania
E-mail: rizea@theory.nipne.ro
[2] *Centre d'Etudes Nucleaires de Bordeaux - Gradignan,*
UMR 5797, CNRS/IN2P3 - Universite Bordeaux 1,
BP 120, 33175 Gradignan Cedex, France
E-mail: carjan@cenbg.in2p3.fr

(Received September 12, 2007)

Abstract. The most intuitive and direct way to study proton emission from unbound nuclear states is to start with a proton wave packet localized inside the well of the p-nucleus interacting potential and follow its time evolution by solving numerically the time-dependent Schrödinger equation (TDSE). Then the physical properties of the decaying system can be inferred from its solution. The most important calculable quantities are: the tunneling probability and the decay rate. In the present paper we consider bi-dimensional axially symmetric nuclear shapes, allowing the treatment of both spherical and deformed nuclei. The solution of TDSE is obtained by the Crank-Nicolson method. We discuss also the treatment of numerical boundary conditions, the preparation of the initial wave function as a quasi-stationary state and the calculation of the decay rate using the flux. In application we reveal the influence of the deformation on the decay rate.

Key words: proton emission, axially deformed nuclei, Cassini parametrization of the nuclear shape, nuclear, spin-orbit and Coulomb potentials, two component wave functions, Crank-Nicolson method, gradient method, transparent boundary conditions, decay rate.

1. INTRODUCTION

The proton emission, a typical example of quantum tunneling, is a dynamical process, with a temporal evolution, and therefore its best description is by TDSE. The time-dependent approach is more exact than the stationary approximations (Wentzel-Kramers-Brillouin and Distorted Wave Born Approximation), widely

used in the past and can be applied in situations for which no alternative methods exist, like the tunneling through a time dependent barrier. This approach was successfully applied to alpha decay and proton emission in an one-dimensional model (see [1–5]). In the present paper we have extended our experience to more realistic models, namely two dimensional potential barriers, in order to treat spherical as well as deformed nuclei.

To solve the time-dependent Schrödinger equation in cylindrical coordinates we have coupled a stable and accurate method for propagation (Crank-Nicolson) with an adequate numerical boundary condition (Transparent Boundary Condition) which avoids the reflections to the numerical (finite) boundaries and allows reasonable large grids. To apply the Crank-Nicolson scheme the derivatives from the Hamiltonian are approximated by finite differences and then we have to solve at each time step a sparse linear system of usually large size (depending on the number of grid points). This is done by a special iterative method, namely the Biconjugate Gradient Method. The initial solution (at $t = 0$) is obtained by solving an eigenvalue problem resulting by the discretization of the stationary Schrödinger equation in two dimensions with a modified potential. For this we have used the package ARPACK (based on the Implicitly Restarted Method of Arnoldi) which solves algebraic eigenvalue problem for large sparse matrices.

The numerical solution of TDSE was used to study the proton decay of different nuclei. Physical quantities such as total tunneling probability and total decay rate have been computed. The decay rate is defined in terms of the derivative of the time dependent tunneling probability. A special procedure was deduced to calculate this derivative using the flux along an equipotential curve.

Our approach is quite general and can be applied to study the temporal behaviour of various atomic, molecular and nuclear phenomena.

2. BI-DIMENSIONAL TIME-DEPENDENT SCHRÖDINGER EQUATION

It has the form

$$i\hbar \frac{\partial \Psi}{\partial t} = \mathcal{H} \Psi \tag{2.1}$$

where $\hbar$ is the Planck constant. The Hamiltonian $\mathcal{H}$ includes the Laplacean, the nuclear potential, the spin-orbit coupling and the Coulomb potential.

The nuclear shape is assumed to be axially symmetric (without other constraints) and cylindrical coordinates will be used. The description of the shape is based on the Cassini parametrization.

The wavefunction has two components, corresponding to spin “up” and spin “down” as follows

$$\Psi = f(\rho, z, t)e^{i\Lambda_1\phi}\,|\uparrow> + g(\rho, z, t)e^{i\Lambda_2\phi}\,|\downarrow>,$$
$$\Lambda_1 = \Omega - \frac{1}{2}, \quad \Lambda_2 = \Omega + \frac{1}{2}. \tag{2.2}$$

Ω is the projection of the total angular momentum along the symmetry axis (z-axis). The Hamiltonian has also two components, H_1 and H_2:

$$H_1\Psi = O_1 f - 2K(S_a g + S_c f)\,|\uparrow>, \tag{2.3}$$

$$H_2\Psi = O_2 g - 2K(S_b f + S_d g)\,|\downarrow> \tag{2.4}$$

where K is a constant and

$$O_1 = -\frac{\hbar^2}{2\mu}\left(\Delta - \frac{\Lambda_1^2}{\rho^2}\right) + V(\rho, z), \quad O_2 = -\frac{\hbar^2}{2\mu}\left(\Delta - \frac{\Lambda_2^2}{\rho^2}\right) + V(\rho, z)$$

with

$$\Delta = \frac{1}{\rho}\frac{\partial}{\partial\rho} + \frac{\partial^2}{\partial\rho^2} + \frac{\partial^2}{\partial z^2},$$
$$S_a = \frac{\partial V}{\partial\rho}\frac{\partial}{\partial z} - \frac{\partial V}{\partial z}\left(\frac{\partial}{\partial\rho} + \frac{\Lambda_2}{\rho}\right), \quad S_b = -\frac{\partial V}{\partial\rho}\frac{\partial}{\partial z} + \frac{\partial V}{\partial z}\left(\frac{\partial}{\partial\rho} - \frac{\Lambda_1}{\rho}\right),$$
$$S_c = \frac{\partial V}{\partial\rho}\frac{\Lambda_1}{\rho}, \quad S_d = -\frac{\partial V}{\partial\rho}\frac{\Lambda_2}{\rho}.$$

μ is the reduced mass.

3. DESCRIPTION OF THE NUCLEAR SHAPE

We have chosen the description based on Cassinian ovals, very convenient for deformed nuclear shapes. In the Cassini parametrization an axially deformed shape is described in cylindrical coordinates by the relations (see Refs. [6, 7]):

$$\bar{\rho} = \frac{1}{\sqrt{2}}\left[P(x) - R^2(x)(2x^2 - 1) - \epsilon R_0^2\right]^{1/2} \tag{3.1}$$

$$\bar{z} = \frac{sign(x)}{\sqrt{2}}\left[P(x) + R^2(x)(2x^2 - 1) + \epsilon R_0^2\right]^{1/2} \tag{3.2}$$

where $P(x) = \left[R^4(x) + 2\epsilon R_0^2(2x^2 - 1) + \epsilon^2 R_0^4\right]^{1/2}$, ϵR_0^2 is the squared distance from the focus of Cassinian ovals to the origin of coordinates and $-1 \le x \le 1$. The function $R(x)$ is represented as a series in Legendre polynomials:

$$R(x) = R_0\left[1 + \sum_{m\geq 1} \alpha_m P_m(x)\right]. \tag{3.3}$$

The set of parameters (ϵ, α_m) determines the nuclear shape.

For applications, the following coordinate transformations are performed: $\overline{\rho} = c\rho$, $\overline{z} = cz + \overline{z}_m$. The scaling factor c is determined by the requirement that the volume enclosed by the surface is constant, independent of nuclear deformation (expressing the incompressibility of nuclear matter), while the displacement $\overline{z}_m$ results by fixing the center of mass at the origin.

4. DEFINITION OF THE POTENTIAL

Let us consider the function

$$\Phi(\rho, z) = \left[(\overline{z}^2 + \overline{\rho}^2)^2 - 2\epsilon R_0^2(\overline{z}^2 - \overline{\rho}^2) + \epsilon^2 R_0^4\right]^{1/4} - R_0\left[1 + \sum_{m\geq 1} \alpha_m P_m(x)\right].$$

The equation $\Phi(\rho, z) = 0$ defines the nuclear surface in cylindrical coordinates. The nuclear potential is given by

$$V = -V_0\left[1 + \exp(\Theta/a)\right]^{-1} \tag{4.1}$$

where V_0 is the depth and a the diffuseness. The quantity Θ is an approximation to the distance between a point and the nuclear surface, given by the expression: $\Theta(\rho, z) = \Phi/|\nabla\Phi|$ (see Ref. [7]).

The form of the nuclear boundary is chosen in such a way that at $\epsilon = 0$, the potential (4.1) turns into the Woods-Saxon potential of the spherical nucleus.

The spin-orbit interaction is taken proportional to the gradient of the potential (4.1):

$$V_{so} = -K[\overline{\boldsymbol{\sigma}} \times \overline{\boldsymbol{p}}]\nabla V, \quad K = \lambda\left(\frac{\hbar}{2\mu c}\right)^2 \tag{4.2}$$

where $\overline{\boldsymbol{\sigma}}$ and $\overline{\boldsymbol{p}}$ are the nucleon spin and momentum. Transforming to cylindrical coordinates (ρ, z, ϕ) and using the assumed axial symmetry in the form $\partial V/\partial\phi = 0$ we find $V_{so} = -(K/2)S$ where

$$S = \sigma^+ e^{-i\phi}\left\{\frac{\partial V}{\partial\rho}\frac{\partial}{\partial z} - \frac{\partial V}{\partial z}\left[\frac{\partial}{\partial\rho} + \frac{1}{\rho}\left(-i\frac{\partial}{\partial\phi}\right)\right]\right\} + \sigma^- e^{i\phi}$$
$$\left\{-\frac{\partial V}{\partial\rho}\frac{\partial}{\partial z} + \frac{\partial V}{\partial z}\left[\frac{\partial}{\partial\rho} - \frac{1}{\rho}\left(-i\frac{\partial}{\partial\phi}\right)\right]\right\} + 2\sigma_z\frac{\partial V}{\partial\rho}\frac{1}{\rho}\left(-i\frac{\partial}{\partial\phi}\right).$$

Here $\sigma^{\pm} = \sigma_x \pm i\sigma_y$, σ_x, σ_y, σ_z being the Pauli matrices:

$$\sigma_x = \begin{pmatrix} 0 & 1 \\ 1 & 0 \end{pmatrix}, \quad \sigma_y = \begin{pmatrix} 0 & -i \\ i & 0 \end{pmatrix}, \quad \sigma_z = \begin{pmatrix} 1 & 0 \\ 0 & -1 \end{pmatrix}.$$

Applied to functions of the mentioned form (up + down) this gives rise to the additional terms in the Hamiltonians (see also Ref. [8]).

The Coulomb potential is assumed to be that of the nuclear charge equal to $(Z-1)e$ and uniformly distributed inside the surface. It is computed using the expression (Ref. [7]):

$$\begin{aligned} V_{coul}(\rho', z') &= \pi\kappa_0 \int_{z_L}^{z_R} M^{-1}(a,b)\left[f + g\frac{d\rho(z)}{dz} \right] dz = \\ &= \pi\kappa_0 \int_{-1}^{1} dx M^{-1}(a,b)\left[\left(f\frac{\partial z}{\partial x} + g\frac{\partial \rho}{\partial x} \right) + \left(f\frac{\partial z}{\partial R} + g\frac{\partial \rho}{\partial R} \right)\frac{dR}{dx} \right] \end{aligned} \tag{4.3}$$

where

$$f = \rho^2(z) + \rho'\rho(z) - \frac{1}{2}Q(a,b), \qquad g = (z'-z)\rho(z),$$

$$a(\rho, z) = \sqrt{(\rho'+\rho)^2 + (z'-z)^2}, \qquad b(\rho, z) = \sqrt{(\rho'-\rho)^2 + (z'-z)^2},$$

$$\kappa_0 = \frac{3(Z-1)e}{4\pi R_0^3}$$

$$\rho = \overline{\rho}/c, \qquad z = (\overline{z} - \overline{z}_m)/c.$$

$M(a, b)$ and $Q(a, b)$ are the elliptic integrals of the first and the second kind. It is implied that $\overline{\rho}$ and $\overline{z}$ are expressed in terms of x and $R(x)$ by formulae (3.1), (3.2).

5. NUMERICAL SOLUTION OF TDSE

We have used the Crank-Nicolson method, extended to two spatial dimensions. It is defined by the relation

$$\left(1 + \frac{i\Delta t}{2\hbar}\mathcal{H}\right)\Psi(t+\Delta t) = \left(1 - \frac{i\Delta t}{2\hbar}\mathcal{H}\right)\Psi(t) \tag{5.1}$$

where Δt is the time step. As known, this method has the advantage to be unconditionally stable and unitary, conserving the norm and the energy (see *e.g.*, [9]). To apply the scheme the numerical domain is discretized by a grid with the mesh points:

$$\rho_j = \left(j - \frac{1}{2}\right)\Delta\rho, \quad j = 1, \ldots, N_\rho, \qquad z_k = k\Delta z, \quad k = -N_z, \ldots, N_z \tag{5.2}$$

(the singularity at $\rho = 0$ of the Hamiltonian was considered). At each point the partial derivatives appearing in $\mathcal{H}$ are approximated by finite difference formulae. Denoting $\Psi_{jk}^{(n)}$ the approximation of Ψ in the point (ρ_j, z_k) and at the moment $t_n = n\Delta t,$ on the basis of Crank- Nicolson scheme the solution $\Psi_{jk}^{(n+1)}$ is obtained in terms of the solution $\Psi_{jk}^{(n)}$ from a linear system. The system matrix has a sparse structure and is usually large (its order is $2 \times N_\rho \times (2N_z + 1),$ since at each node of the grid correspond two values: *f* and *g*). If one considers the matrix as full or even band, to apply direct methods of solving linear systems (like Gaussian elimination or LU decomposition), difficulties related to memory size and computing time will appear. We prefered to use an iterative method, namely the biconjugate gradient method – BCG (see [9]). The attractiveness of this method for large sparse systems is that it references the system matrix only through its multiplication by a vector, thus avoiding the storage of the matrix.

Given the system **Ax = b**, the idea is to minimize the function

$$h(\mathbf{x}) = \frac{1}{2}\mathbf{x}\mathbf{A}\mathbf{x} - \mathbf{b}\mathbf{x}. \tag{5.3}$$

This function is minimized when its gradient $\nabla h = \mathbf{A}\mathbf{x} - \mathbf{b}$ is zero, which is equivalent to the original system. The minimization is carried out by generating a succession of vectors $\mathbf{p}_k$ and $\mathbf{x}_k$. At each stage a quantity α_k is found that minimizes $h(\mathbf{x}_k + \alpha_k \mathbf{p}_k)$ and the iteration $\mathbf{x}_{k+1}$ is set equal to $\mathbf{x}_k + \alpha_k \mathbf{p}_k$. In our calculations we have used a routine in double complex arithmetic based on an optimized BCG algorithm (see Ref. [10]).

6. TRANSPARENT BOUNDARY CONDITIONS

For numerical treatment the spatial domain should be finite, but sufficiently large to avoid the reflexions on the numerical boundaries which affect the propagated wave function and lead to errors in the calculation of the physical quantities. By using a special boundary condition algorithm – namely Transparent Boundary Conditions, the grid can be reduced and consequently, the computer time. To recall the TBC algorithm, let us consider the TDSE in one dimensional spatial coordinate:

$$i\hbar \frac{\partial f}{\partial t} = -\frac{\hbar^2}{2\mu}\frac{\partial^2 f}{\partial x^2} + V(x) f \tag{6.1}$$

restricted to the computational domain [*a*, *b*]. We assume that near the boundary *b* the solution has the form: $f = f_0 \exp(ik_x x),$ where f_0 and k_x are complex constants

(see [11]). Let be $x_0 = a,\ x_1 = a + \Delta x,\ \ldots,\ x_j = a + j\Delta x,\ \ldots, x_M = b$ the partition of the interval $[a, b]$. When the Crank-Nicolson scheme is applied, we adjust the boundary value f_{M+1}^n (which enters into the approximation of $f''(x_M)$ and without TBC is assumed to be 0) from the relation

$$\frac{f_{M+1}^n}{f_M^n} = \frac{f_M^n}{f_{M-1}^n} = \exp(ik_x \Delta x). \tag{6.2}$$

The value of k_x is determined from the second equality; then f_{M+1}^n can be expressed in terms of f_M^n. Assuming the same relation valid for the new time step, we have

$$f_{M+1}^{n+1} = f_M^{n+1} exp(ik_x \Delta x). \tag{6.3}$$

An important feature of the above procedure is that k_x is allowed to change as the problem progresses, thus eliminating the need for a problem-dependent adjustable parameter.

This algorithm can also be applied in two spatial dimensions. In this case the value of k_x is different at each mesh point belonging to the boundaries. For our problem the transparent boundary conditions are applied on the row (ρ_M, z_j), $j = 1, 2, \ldots, N$ and columns (ρ_i, z_1), $i = 1, 2, \ldots, M$, respectively (ρ_i, z_N) $i = 1, 2, \ldots, M$ (M is the number of points in ρ direction and N is the number of points in z direction).

7. APPLICATIONS

The numerical solution of TDSE was used to study the proton decay of spherical and deformed nuclei. The following physical quantitites are computed:

1. **Total tunneling probability** given by the fraction of the wave function located beyond the top of the two dimensional potential barrier (potential ridge) at time t:

$$P_{tun}(t) = 2\pi \int_{D_{ext}} |\Psi(\rho, z, t)|^2 \, \rho d\rho dz \tag{7.1}$$

2. **Total decay rate** related to the total tunneling probability by

$$\lambda(t) = \frac{1}{N_{tot} - P_{tun}} \frac{dP_{tun}(t)}{dt} \tag{7.2}$$

where N_{tot} is the total norm given by

$$N_{tot}(t) = 2\pi \int_D |\Psi(\rho, z, t)|^2 \, \rho d\rho dz \tag{7.3}$$

3. **Mean value** of L^2, defined as

$$< L^2 > (t) = < \Psi(t) | L^2 | \Psi(t) > = < l > (t)[< l > (t) + 1] \tag{7.4}$$

with the operator L^2 written in cylindrical coordinates as

$$L^2 = -\left[\left(z\frac{\partial}{\partial \rho} - \rho \frac{\partial}{\partial z} \right)^2 + \frac{z^2}{\rho}\frac{\partial}{\partial \rho} - z\frac{\partial}{\partial z} - \Lambda^2 \left(1 + \frac{z^2}{\rho^2} \right) \right]. \tag{7.5}$$

When the potential is spherical, this operator commutes with the Hamiltonian and the quantity $< L^2 >$ is a constant of the motion, giving rise to the centrifugal potential.

4. **Energy** of the system, according to

$$E = 2\pi \int f^* H \Psi \rho d\rho dz / N_{tot}. \tag{7.6}$$

In practice, $N_{tot} - P_{tun}$ is replaced by

$$N_{int}(t) = 2\pi \int_{D_{int}} |\Psi(\rho, z, t)|^2 \, \rho d\rho dz \tag{7.7}$$

which is more convenient for calculations. The domain D_{int} is delimited by the equipotential curve corresponding to the energy of the system and the axis $\rho = \rho_{min}$, while the domain D_{ext} is the complementary of D_{int} with respect to D.

8. THE DERIVATIVE OF $P_{tun}(t)$

The evaluation of $dP_{tun}(t)/dt$ requires a special attention. One way would be to evaluate the two-dimensional integral on the domain D_{ext} and then numerically obtain the derivative with respect to time. But, apart the difficulty to calculate an integral in two dimensions, the entire wavefunction outside the numerical domain will be neglected. This introduces a crude approximation which can spoil the value of λ. A simpler and more accurate method to calculate dP_{tun}/dt is by the **flux**, as will be shown in the following. The regions of interest are drawn in the Fig. 1.

Let us consider $p(r, t) = |\Psi(r, t)|^2$, called **the probability density** (r stands for spatial coordinate vector). We have

$$\frac{\partial p}{\partial t} = \frac{\partial (\Psi \Psi^*)}{\partial t} = \Psi^* \frac{\partial \Psi}{\partial t} + \Psi \frac{\partial \Psi^*}{\partial t}.$$

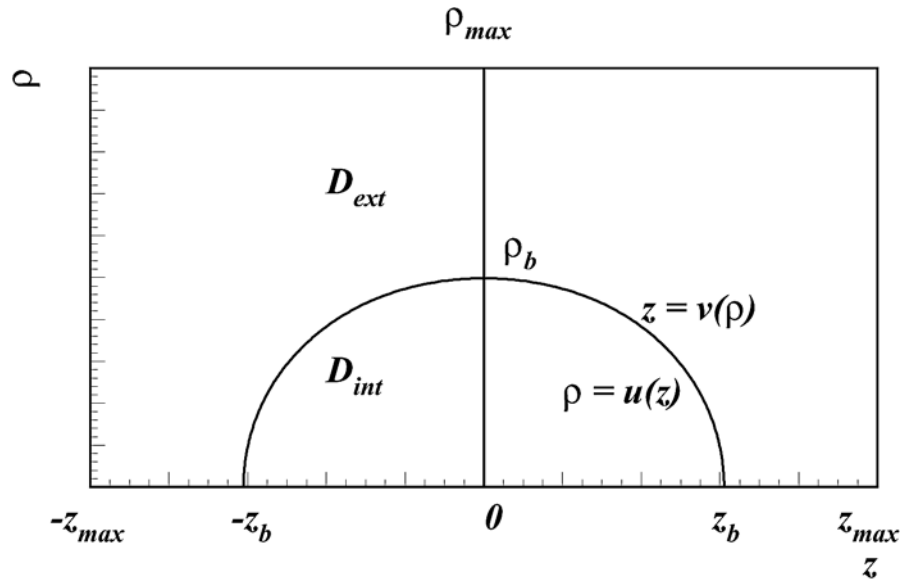

Fig. 1 – Regions implied in the calculation of $P'_{tun}(t)$.

From the Schrödinger equation

$$i\hbar\frac{\partial\Psi(r,t)}{\partial t}=-\frac{\hbar^2}{2\mu}\Delta\Psi(r,t)+V(r)\Psi(r,t) \tag{8.1}$$

and its complex conjugate one obtains

$$\frac{\partial p}{\partial t}=\frac{i}{\hbar}\frac{\hbar^2}{2\mu}(\Psi^*\Delta\Psi-\Psi\Delta\Psi^*). \tag{8.2}$$

We note

$$J(r,t)=-\frac{i}{\hbar}\frac{\hbar^2}{2\mu}(\Psi^*\nabla\Psi-\Psi\nabla\Psi^*). \tag{8.3}$$

J is called **the current density**. The expression

$$\nabla J(r,t)=divJ(r,t)=-\frac{i}{\hbar}\frac{\hbar^2}{2\mu}(\Psi^*\Delta\Psi-\Psi\Delta\Psi^*) \tag{8.4}$$

represents **the flux**. From Eq. (8.2) it results:

$$\frac{\partial p}{\partial t}+\nabla J=0 \tag{8.5}$$

which is called **the continuity equation** (see [12]). We shall use the continuity equation in cylindrical coordinates. We have

$$J = -\frac{i}{\hbar}\frac{\hbar^2}{2\mu}\left[\left(\Psi^*\frac{\partial\Psi}{\partial\rho} - \Psi\frac{\partial\Psi^*}{\partial\rho}\right)\overline{e}_\rho + \left(\Psi^*\frac{\partial\Psi}{\partial z} - \Psi\frac{\partial\Psi^*}{\partial z}\right)\overline{e}_z\right],$$

$$\nabla J = \frac{1}{\rho}\frac{\partial}{\partial\rho}\left(\rho J_\rho\right) + \frac{\partial}{\partial z}J_z =$$

$$-\frac{i}{\hbar}\frac{\hbar^2}{2\mu}\left\{\frac{1}{\rho}\frac{\partial}{\partial\rho}\left[\rho\left(\Psi^*\frac{\partial\Psi}{\partial\rho} - \Psi\frac{\partial\Psi^*}{\partial\rho}\right)\right] + \frac{\partial}{\partial z}\left(\Psi^*\frac{\partial\Psi}{\partial z} - \Psi\frac{\partial\Psi^*}{\partial z}\right)\right\}.$$

Taking now into account the continuity equation, we have successively:

$$\begin{aligned}\frac{dP_{tun}(t)}{dt} &= -2\pi\int_{D_{ext}}\nabla J\rho d\rho dz = \\ &= 2\pi\frac{i}{\hbar}\frac{\hbar^2}{2\mu}\left(\int_{D_{ext}}\frac{\partial P}{\partial\rho}d\rho dz + \int_{D_{ext}}\frac{\partial Q}{\partial z}d\rho dz\right) = 2\pi\frac{i}{\hbar}\frac{\hbar^2}{2\mu}(I_1 + I_2),\end{aligned} \tag{8.6}$$

where

$$P(\rho, z) = \rho\left(\Psi^*\frac{\partial\Psi}{\partial\rho} - \Psi\frac{\partial\Psi^*}{\partial\rho}\right), \quad Q(\rho, z) = \rho\left(\Psi^*\frac{\partial\Psi}{\partial z} - \Psi\frac{\partial\Psi^*}{\partial z}\right).$$

We consider now the domain D_{ext}. It is delimited by the equipotential line (defined as the most exterior curve on which $V(\rho, z) = E$) and the limits of the numerical domain. The same equipotential line can be expressed either as $\rho = u(z)$ or as $z = v(\rho)$. Using the notations in Fig. 1 and some mathematical rules of integral theory, we obtain:

$$\begin{aligned}I_1 &= \int_{-z_{max}}^{-z_b} dz\int_{\rho_1}^{\rho_M}\frac{\partial P}{\partial\rho}d\rho + \int_{-z_b}^{z_b} dz\int_{\rho=u(z)}^{\rho_M}\frac{\partial P}{\partial\rho}d\rho + \int_{z_b}^{z_{max}} dz\int_{\rho_1}^{\rho_M}\frac{\partial P}{\partial\rho}d\rho = \\ &= \int_{-z_{max}}^{-z_b}\left[P(\rho_M, z) - P(\rho_1, z)\right]dz + \int_{-z_b}^{z_b}\left[P(\rho_M, z) - P(u(z), z)\right]dz + \\ &\quad + \int_{z_b}^{z_{max}}\left[P(\rho_M, z) - P(\rho_1, z)\right]dz.\end{aligned}$$

$-z_b$ and z_b are the points where the equipotential curve crosses the line $\rho = \rho_1$. When the considered case has a symmetry with respect to $z = 0$, we can limit ourselves to a half of domain. Thus, for the configuration in Fig. 1 we have

$$\frac{1}{2}I_1 = \int_0^{z_b}\left[P(\rho_{max}, z) - P(u(z), z)\right]dz + \int_{z_b}^{z_{max}}\left[P(\rho_{max}, z) - P(\rho_1, z)\right]dz,$$

$$\begin{aligned}\frac{1}{2}I_2 &= \int_{\rho_1}^{\rho_b} d\rho\int_{z=v(\rho)}^{z_{max}}\frac{\partial Q}{\partial z}dz + \int_{\rho_b}^{\rho_{max}} d\rho\int_0^{z_{max}}\frac{\partial Q}{\partial z}dz = \\ &= \int_{\rho_1}^{\rho_b}\left[Q(\rho, z_{max}) - Q(\rho, v(\rho))\right]d\rho + \int_{\rho_b}^{\rho_{max}}\left[Q(\rho, z_{max}) - Q(\rho, 0)\right]d\rho.\end{aligned}$$

ρ_b is the point where the equipotential curve meets the axis $z = 0$. Now, the terms containing the values ρ_{max} and z_{max}, belonging to the boundaries, are considered zero, since theoretically ρ_{max}, z_{max} tend to ∞ and there the wavefunction should be zero. It results:

$$\frac{1}{2} I_1 = -\int_0^{z_b} P(u(z), z)dz - \int_{z_b}^{z_{max}} P(\rho_1, z)dz, \tag{8.7}$$

$$\frac{1}{2} I_2 = -\int_{\rho_1}^{\rho_b} Q(\rho, v(\rho))d\rho - \int_{\rho_b}^{\rho_{max}} Q(\rho, 0)d\rho. \tag{8.8}$$

Thus, the only values which we are obliged to neglect in the numerical calculation are $\Psi(\rho_1, z)$, $z > z_{max}$ and $\Psi(\rho, 0)$, $\rho > \rho_{max}$, which normally are small. With the notations

$$\Psi = a + ib, \quad \frac{\partial \Psi}{\partial \rho} = a_\rho + ib_\rho, \quad \frac{\partial \Psi}{\partial z} = a_z + ib_z$$

we have:

$$P(\rho, z) = 2i\rho(ab_\rho - a_\rho b), \quad Q(\rho, z) = 2i\rho(ab_z - a_z b).$$

Using the equations (8.7), (8.8) one can obtain I_1, I_2 and then $dP_{tun}(t)/dt$ from equation (8.6) (its value is strictly real). Of course, in practice the equipotential curve, the first derivatives with respect to ρ, z and the uni-dimensional integrals are evaluated numerically, using the values at grid points.

9. RESULTS

We have first investigated the case of proton emission from ground state of I^{109}, considered as a spherical nucleus. The initial wave function was produced on a grid of dimensions 513×1025 using a spatial step equal to 1/4 (so that $0.125 \le \rho \le 128.125$, $-128 \le z \le 128$). It was obtained by solving the stationary Schrödinger equation in two dimensions with a modified potential (set equal to some constant value beyond some distance). After the discretization of the equation $\mathcal{H}\Psi = E\Psi$ by finite difference formulae, one arrives to an algebraic eigenvalue problem. This was solved by using the package ARPACK (based on the implicitly restarted method of Arnoldi) conceived for eigenvalue problems with large sparse matrices (see [13]).

The depth of the nuclear potential is adjusted to give an eigenenergy equal to the experimental value Q_p. The index n_{ev} of the eigenvalue corresponds to the level from which the proton is emitted (in our case $n_{ev} = 6$). The modified potential (nuclear + coulomb) is shown in the upper half of Fig. 2. In Fig. 3 it is represented

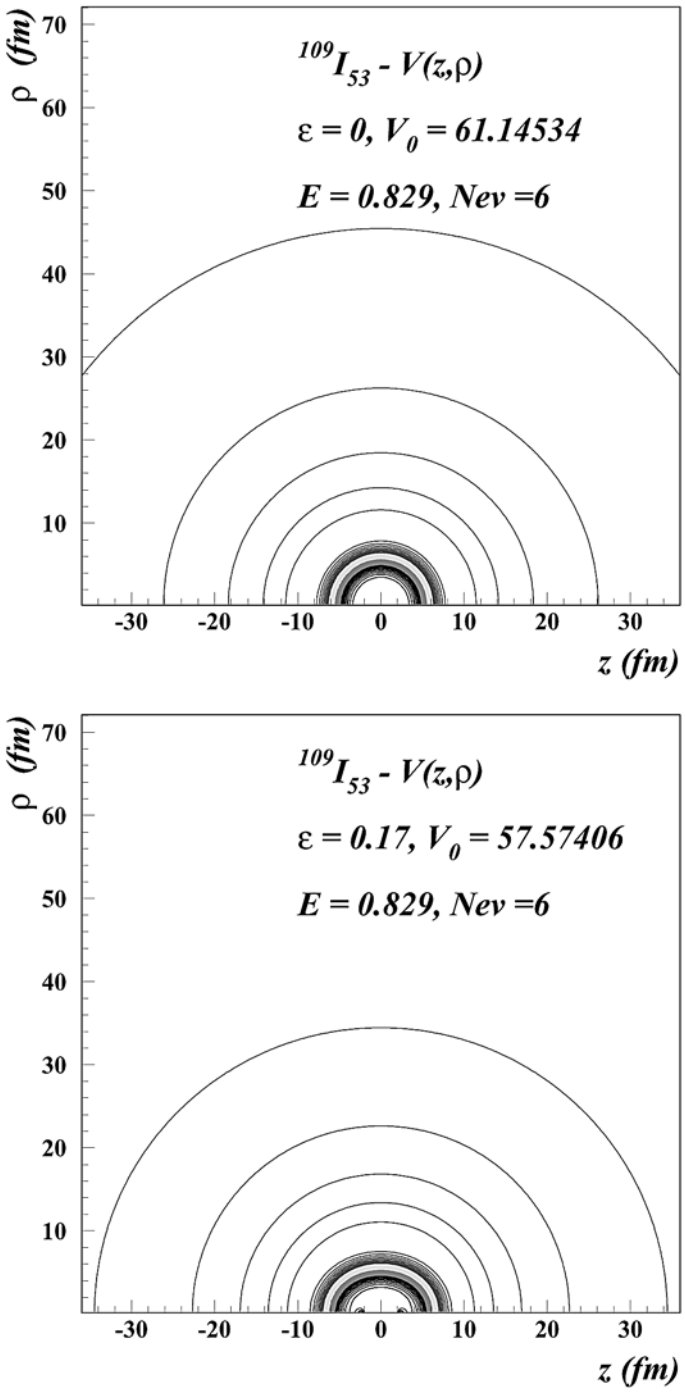

Fig. 2 – Potentials – spherical and deformed.

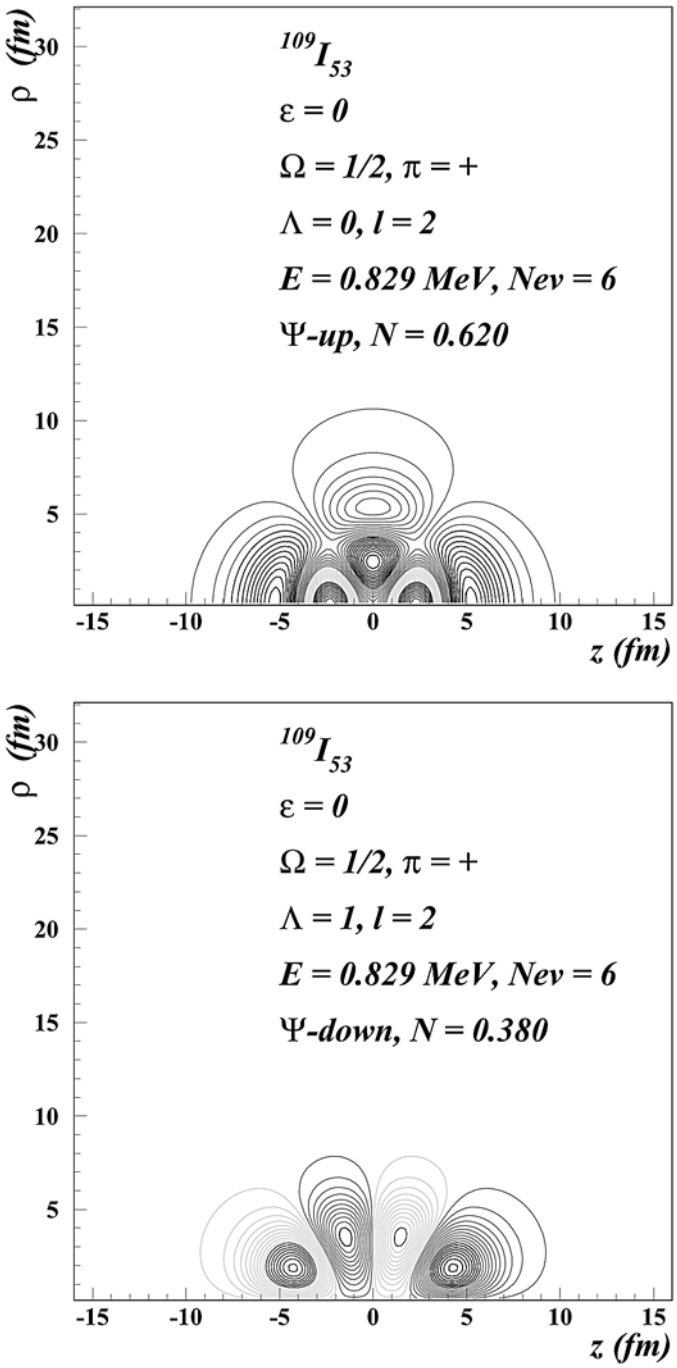

Fig. 3 – Initial w.f. – up and down (spherical).

the eigenfunction corresponding to the eigenenergy $E = 0.829$ MeV (both components). The next step consists in inserting this state as initial wavefunction in TDSE with the original Hamiltonian and in calculating its time evolution. For TDSE solving, the grid have to be increased by a factor in both directions to avoid numerical reflexions. Using of TBC allows a remarkable small factor. For our example it was 2. Thus, the number of points in which the solution has to be computed was $2 * 513 \times 2 * 1025$. The initial wavefunction is set 0 in the additional points of the extended grid. When the Crank-Nicolson scheme was applied, we found that a time step $\Delta t = 1/32$ (in units of 10^{-22} s) ensures the convergence of the gradient method in an acceptable number of iterations (of order 15 for a tolerance of 10^{-15}).

In Fig. 5 we present a typical evolution of the decay rate. It increases with oscillations until a maximum and then decreases exponentially. The first stage corresponds to the "aclimatization" of the particle state to the real Hamiltonian, since the initial wavefunction is prepared as an eigenstate of the modified Hamiltonian. Finally, the decay rate reaches an *asymptotic* value, denoted by λ_∞, from which the half-life time can be obtained by the formula $t_{1/2} = ln2/\lambda_\infty$. In our case, the asymptotic value of the decay rate was $\lambda_\infty = 0.689 \times 10^5$ s^{-1}, which gives $t_{1/2} = 10$ μs. We note that the result was also compared with the decay rate obtained through the one-dimensional time-dependent model, which is possible in the spherical case. The agreement is rather good (4 decimal digits), which validates the bidimensional model. Note that the same value of half-life has been obtained, in an one-dimensional stationary approach, by DWBA approximation (see [14]). The value of $< l >$ obtained from the mean value operator is 2 (constant during the evolution in time). It was also verified that the norm and the energy are conserved, this being a property of the Crank-Nicolson scheme.

Next we present results for the deformed case. We have considered the same nucleus, reported as deformed in [15]. Thus, one can see the effect of the deformation. In the lower part of Fig. 2 it is represented the potential corresponding to the ε deformation of 0.17 (this is approximately the equivalent of the deformation given in [15] using β parametrization). The two components of the initial wavefunction are shown in Fig. 4. The resulting decay rate appears in the upper half of Fig. 6 together with the rate obtained in the spherical assumption. The value of λ_∞ is greater in the deformed case (2.460×10^5 s^{-1} compared to 0.689×10^5 s^{-1}). The rates are of course influenced by the values of the nuclear depth used to obtain the same value (Q_p) of the energy. It was necessary to take different values for V_0: 61.14 for the spherical nucleus and 57.57 for the deformed nucleus. But mainly the difference in the asymptotic values of λ can be explained by the barrier width, smaller when the potential is deformed. In the lower half of Fig. 6 we represented the equipotential lines corresponding to the maximum of the

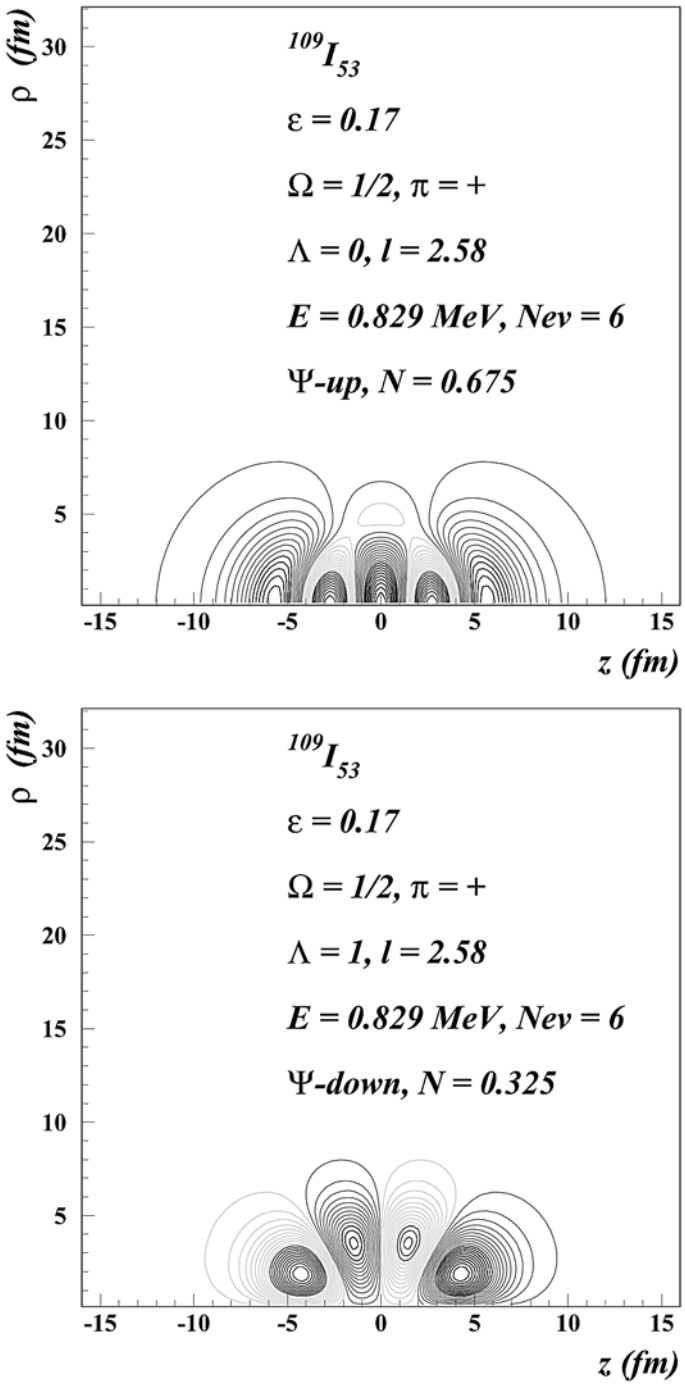

Fig. 4 – Initial w.f. – up and down (deformed).

potential in both cases. The deformed potential reaches its maximum at smaller distance along the symmetry axis. Also, the distance between the turning points is different. We have evaluated it on the two axes (for $z \geq 0$). In the spherical case, we have obtained the same value in both directions: 83.54, while in the deformed case we got 83.92 on the line $z = 0$ and 82.96 on the line $\rho = \rho_1$. As known, the decay rate depends on the volume enclosed by the potential and the plane situated at the height of the energy. A smaller volume gives a greater λ. In the one-dimensional model, the equivalent is the area A delimited by the potential and the energy. According to WKB approximation, the decay rate is proportional to $\exp(-A)$ (see [14]). For the deformed case, the resulting life-time is $t_{1/2}^{th} = 2.46\,\mu s$. The experimental value is $t_{1/2}^{exp} = 100\,\mu s$ (see [15]). In order to obtain the experimental value, one has to multiply the theoretical value of λ by the so called spectroscopic factor S_p. It represents the fragmentation probability and can be calculated in the frame of Bardeen-Cooper-Schrieffer theory (or others). In principle, S_p should be close to the ratio $t_{1/2}^{th}/t_{1/2}^{exp}$. Finally, we note that the value of $< l >$ given by the mean value operator remains constant also in the deformed case, but is no more an integer: its value is 2.58.

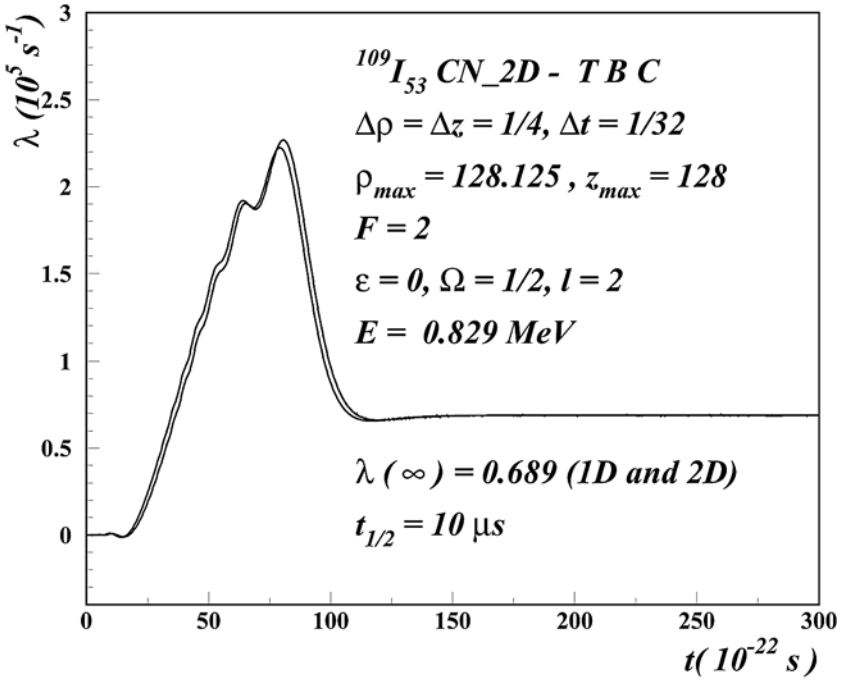

Fig. 5 – Decay rates – spherical (1D,2D).

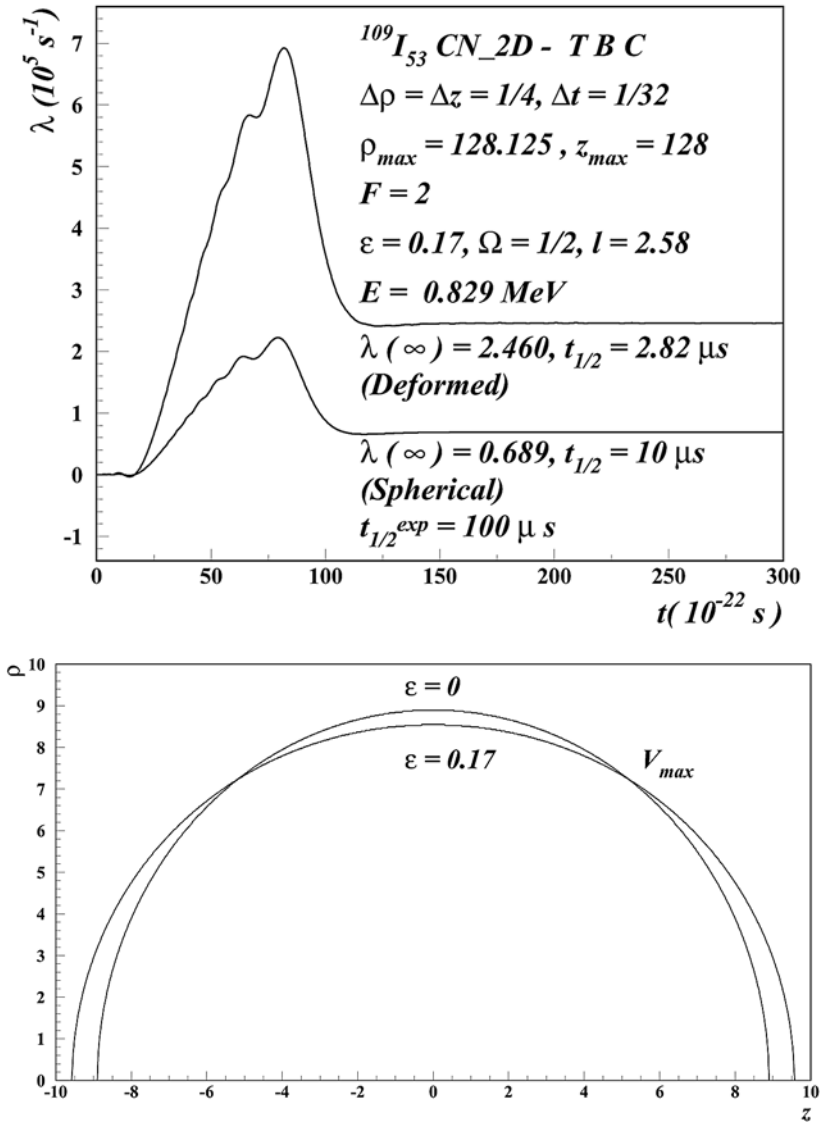

Fig. 6 – Decay rates – spherical + deformed and the top equipotential lines.

10. CONCLUSION

In this paper, we have presented numerical procedures to solve the time-dependent Schrödinger equation with application to the proton emission. In order to study deformed nuclei we have used cylindrical coordinates. The approximate solution of TDSE is calculated by the Crank-Nicolson method associated with

Transparent Boundary Conditions. We have obtained stable results with a reasonable amount of grid points and time steps. The linear system resulting after discretization was solved by a special algorithm (of bi-conjugate gradients). We have evaluated physical quantitites as: the tunneling probability, the decay rate, from which results the half-life, the mean value of the operator L^2, the energy of the system during the time propagation, etc. We deduced a special procedure to accurately calculate the derivative of the tunneling probability (involved in the decay rate formula), using the flux along an equipotential curve. The numerical scheme was first used for a spherical nucleus, to allow the comparison with one-dimensional models. The results where satisfactory enough and we considered next a deformed case. The effect of the deformation was also discussed. The time-dependent approach in two spatial dimensions, an intuitive and realistic model of the quantum tunnelling, can be used for a large variety of nuclei. It can offer informations in cases where experimental data are not available or are very difficult to obtain. It can be also applied in other processes, like alpha-decay or the tunnelling through a time-dependent potential barrier.

REFERENCES

1. O. Serot, N. Carjan, D. Strottman, *Transient behaviour in quantum tunneling: time-dependent approach to alpha decay*, Nucl. Phys. A, **569** (1994) 562–574.
2. P. Talou, D. Strottman, N. Carjan, *Exact calculations of proton decay rates from excited states in spherical nuclei*, Phys. Rev. C, **60** (1999) 054318.
3. N. Carjan, P. Talou, M. Rizea, D. Strottman, *Proton-emitting nuclei in a time dependent formalism*, AIP Conference Proceedings 518: Proton-Emitting Nuclei, First International Symposium, Oak Ridge, Tennessee – U.S.A. (2000) 223–226.
4. S. Misicu, M. Rizea, W. Greiner, *Emission of electromagnetic radiation in alpha decay*, J. Phys. G, **27** (2001) 993–1003.
5. N. Carjan, M. Rizea, D. Strottman, *Improved boundary conditions for the decay of low lying metastable proton states in a time-dependent approach*, Comp. Phys. Commun., **173** (2005) 41–60.
6. V. S. Stavinsky, N. S. Rabotnov, A. A. Seregin, Yad. Fiz., **7** (1968) 1051 [Sov. J. Nucl. Phys. **7** (1968) 631].
7. V. V. Pashkevich, *On the asymmetric deformation of fissioning nuclei*, Nucl. Phys. A, **169** (1971) 275–293.
8. J. Damgaard, H. C. Pauli, V. V. Pashkevich, V. M. Strutinsky, *A method for solving the independent-particle Schrödinger equation with a deformed average field*, Nucl. Phys. A, **135** (1969) 432–444.
9. W. H. Press, S. A. Teukolsky, W. T. Vetterling, B. P. Flannery, *Numerical Recipes in Fortran – The Art of Scientific Computing*, Second Edition, Cambridge University Press (1996).
10. M. Botchev, D. Fokkema, *zbcg2.f90 – Improved BiCGstab(l) iterative method*, **www.math.uu.nl/ people/vorst/software.html**, Utrecht University (2001).
11. G. Ronald Hadley, *Transparent boundary conditions for beam propagation*, Optics Letters, **16** (1991) 624–626.
12. C. Cohen-Tannoudji, B. Diu, F. Laloë, *Mécanique Quantique*, Hermann, Paris (1973).
13. D. Sorensen, R. Lehoucq, Chao Yang, K. Maschhoff, *ARPACK – An implementation of the implicitly restarted Arnoldi method for computing a few selected eigenvalues and corresponding eigenvectors of a large sparse matrix*, **www.caam.rice.edu/ software/ARPACK**, Rice University (2001).
14. S. Aberg, P. Semmes, W. Nazarewicz, *Spherical proton emitters*, Phys. Rev. C, **56** (1997) 1762–1773, Phys. Rev. C, **58** (1998) 3011.
15. A. A. Sonzogni, *Proton radioactivity in $Z > 50$ nuclides*, Nuclear Data Sheets, **95** (2002) 1–48.